

Geophysical Research Letters[®]



RESEARCH LETTER

10.1029/2022GL099381

The Hunga Tonga-Hunga Ha'apai Hydration of the Stratosphere

Key Points:

- Following the Hunga Tonga-Hunga Ha'apai eruption, the Aura Microwave Limb Sounder measured enhancements of stratospheric H₂O, SO₂, and HCl
- The mass of SO₂ and HCl injected is comparable to that from prior eruptions, whereas the magnitude of the H₂O injection is unprecedented
- Excess stratospheric H₂O will persist for years, could affect stratospheric chemistry and dynamics, and may lead to surface warming

Supporting Information:

Supporting Information may be found in the online version of this article.

Correspondence to:









L. Millán,
luis.f.millan@jpl.nasa.gov

Citation:

Millán, L., Santee, M. L., Lambert, A., Livesey, N. J., Werner, F., Schwartz, M. J., et al. (2022). The Hunga Tonga-Hunga Ha'apai Hydration of the Stratosphere. *Geophysical Research Letters*, 49, e2022GL099381. <https://doi.org/10.1029/2022GL099381>

Received 30 APR 2022

Accepted 2 JUN 2022

L. Millán¹ , M. L. Santee¹ , A. Lambert¹, N. J. Livesey¹ , F. Werner¹ , M. J. Schwartz¹ , H. C. Pumphrey² , G. L. Manney^{3,4} , Y. Wang^{1,5} , H. Su¹ , L. Wu¹ , W. G. Read¹, and L. Froidevaux¹

¹Jet Propulsion Laboratory, California Institute of Technology, Pasadena, CA, USA, ²School of GeoSciences, The University of Edinburgh, Edinburgh, UK, ³NorthWest Research Associates, Socorro, NM, USA, ⁴New Mexico Institute of Mining and Technology, Socorro, NM, USA, ⁵Division of Geological and Planetary Sciences, California Institute of Technology, Pasadena, CA, USA

Abstract Following the 15 January 2022 Hunga Tonga-Hunga Ha'apai eruption, several trace gases measured by the Aura Microwave Limb Sounder (MLS) displayed anomalous stratospheric values. Trajectories and radiance simulations confirm that the H₂O, SO₂, and HCl enhancements were injected by the eruption. In comparison with those from previous eruptions, the SO₂ and HCl mass injections were unexceptional, although they reached higher altitudes. In contrast, the H₂O injection was unprecedented in both magnitude (far exceeding any previous values in the 17-year MLS record) and altitude (penetrating into the mesosphere). We estimate the mass of H₂O injected into the stratosphere to be 146 ± 5 Tg, or $\sim 10\%$ of the stratospheric burden. It may take several years for the H₂O plume to dissipate. This eruption could impact climate not through surface cooling due to sulfate aerosols, but rather through surface warming due to the radiative forcing from the excess stratospheric H₂O.

Plain Language Summary The violent Hunga Tonga-Hunga Ha'apai eruption on 15 January 2022 not only injected ash into the stratosphere but also large amounts of water vapor, breaking all records for direct injection of water vapor, by a volcano or otherwise, in the satellite era. This is not surprising since the Hunga Tonga-Hunga Ha'apai caldera was formerly situated 150 m below sea level. The massive blast injected water vapor up to altitudes as high as 53 km. Using measurements from the Microwave Limb Sounder on NASA's Aura satellite, we estimate that the excess water vapor is equivalent to around 10% of the amount of water vapor typically residing in the stratosphere. Unlike previous strong eruptions, this event may not cool the surface, but rather it could potentially warm the surface due to the excess water vapor.

1. Introduction

Hunga Tonga-Hunga Ha'apai (HT-HH), a submarine volcano in the South Pacific (20.54°S, 175.38°W), reached its climactic eruption phase on 15 January 2022. The blast sent a volcanic plume into the mesosphere to altitudes of up to 57 km—a record in the satellite era (Carr et al., 2022; Proud et al., 2022). It also triggered tsunami alerts across the world (Carvajal et al., 2022; Ramirez-Herrera et al., 2022), waves that propagated globally (Wright et al., 2022), and ionospheric disturbances (Themens et al., 2022). Details about the HT-HH caldera complex, seismology, and volcanology are given by Kusky (2022) and Yuen et al. (2022).

In addition to particulate matter, volcanic eruptions can loft large quantities of gases into the stratosphere. Although around 80% of this gas volume can be magmatic H₂O (Coffey, 1996; Pinto et al., 1989), up to 90% of the volcanically emitted humidity is usually removed by condensation at the cold point tropopause (Glaze et al., 1997). Considerable amounts of CO₂ and SO₂ are also often found in volcanic plumes, along with HCl and other trace gases (e.g., Carn et al., 2016). SO₂ reacts with H₂O and OH to form submicron sulfate aerosols that reflect solar radiation, lowering surface temperature. For example, the radiative influence of the 1991 Mount Pinatubo eruption “put an end to several years of globally warm surface temperature” (McCormick et al., 1995), illustrating the capacity of volcanic eruptions to substantially alter global climate.

The composition of the HT-HH plume is unprecedented, as the eruption injected vast amounts of H₂O directly into the stratosphere. The high moisture content of the plume is perhaps not surprising since the HT-HH caldera

© 2022 Jet Propulsion Laboratory, California Institute of Technology. Government sponsorship acknowledged. This is an open access article under the terms of the [Creative Commons Attribution-NonCommercial License](https://creativecommons.org/licenses/by-nc/4.0/), which permits use, distribution and reproduction in any medium, provided the original work is properly cited and is not used for commercial purposes.

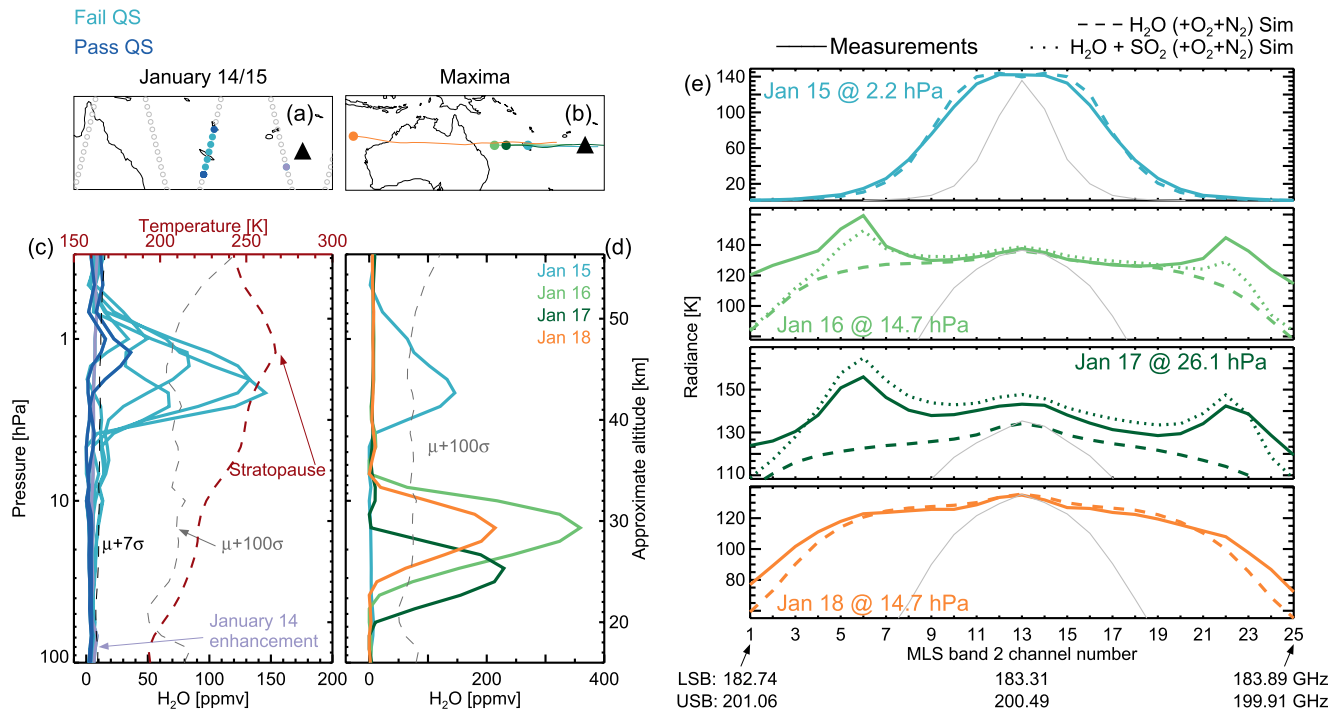


Figure 1. (a) Location of observed H₂O enhancements on 14 and 15 January. (b) Location of maximum H₂O on 15–18 January. Lines display back trajectories from these measurements to the eruption time. Triangles mark the volcano location. (c) H₂O profiles associated with locations shown in (a). The temperature profile (red dashed line) is the average of the temperature profiles retrieved by the Microwave Limb Sounder (MLS) at those locations. (d) H₂O profiles associated with locations shown in (b). The 2005–2021 January–February–March mean plus 100 standard deviation values ($\mu + 100\sigma$) are also shown in (c) and (d). (e) Measured (solid lines) and simulated (with and without considering SO₂, dotted and dashed lines, respectively) radiances at the mixing ratio maxima for the enhanced profiles shown in (d) (colored lines) as well as for background conditions at the same pressure levels (gray lines). Note that this MLS spectrometer is centered on the 183.3 GHz H₂O spectral line. Most MLS spectrometers observe emissions from two separate spectral regions: the “lower sideband” (LSB) and “upper sideband” (USB) as indicated for selected channels.

was situated 150 m below sea level (Cronin et al., 2017), where water in contact with the erupting magma (at temperatures of ~1100–1470 K) was superheated, resulting in explosive steam.

The Microwave Limb Sounder (MLS) onboard NASA's Aura satellite provides measurements of 15 trace gases, among them H₂O, HCl, and enhanced volcanic SO₂. MLS measures thermal emission from the Earth's limb, covering spectral regions near 118, 190, 240, and 640 GHz (Waters et al., 2006). MLS is well suited to observe volcanic plumes since microwave radiances are largely unaffected by sulfate aerosols. Moreover, the MLS two-dimensional retrieval exploits overlapping limb observations to better constrain trace gas gradients (Livesey et al., 2006), allowing the spatial heterogeneity of the plume to be captured.

Here, we use MLS version 4 (v4) data, instead of the most recent version (v5). Estimates of instrument pointing are required for atmospheric composition profile retrievals. V4 obtains pointing purely from O₂ signals, whereas v5 also uses the H₂O line. Poor fits to H₂O signals in regions with extremely enhanced humidity, such as those discussed here, lead to discrepancies in pointing as large as ~2.5 km, degrading the accuracy of some v5 products.

2. Validity of MLS Measurements After the Eruption

Ten hours after the eruption on 15 January, MLS measured enhanced values of H₂O at altitudes up to 0.46 hPa (~53 km), well above the stratopause (Figure 1c). Most of these measurements of enhanced H₂O did not pass the MLS quality screening (QS) criteria defined by Livesey et al. (2020), indicating that the retrieval achieved only a poor fit to the radiances. The poor performance of the standard data processing algorithms is unsurprising, as the largest H₂O values are more than an order of magnitude greater than any previously observed by MLS and more than 100 standard deviations above background levels. Here, data points with values greater than 7 standard deviations above the climatological January–February–March 2005–2021 average are identified as enhancements.

The eruption injected H₂O throughout a large vertical range encompassing most of the stratosphere, but on 15 January, MLS only measured the outer edge of the plume in the upper stratosphere, where strong winds advected the lofted H₂O to locations sampled by MLS. Near 80 hPa on this day, MLS also measured some enhanced H₂O injected by a previous, less violent, HT-HH eruption on 14 January.

For the next several days, most of the largest enhancements failed the QS. Figure 1d shows the profiles displaying the largest mixing ratios on 15, 16, 17, and 18 January. Back trajectories (as in Livesey et al. (2015); Santee et al. (2022)) indicate that these enhancements lie downwind from the HT-HH volcano (Figure 1b), and the measured spectral signature is well represented by radiance simulations (Figure 1e). Peaks centered on channels 5 and 22 on 16 and 17 January are SO₂ spectral lines; they indicate that these lower plumes contained more SO₂ than the high-altitude plume on 15 January.

As the plume dispersed, the daily number of profiles failing the QS increased, reaching a maximum on 19 January. Retrieval performance then returned to normal by 8 February, by which time the plume had dispersed sufficiently that maximum H₂O values had dropped to ~50 ppmv, versus up to 350 ppmv immediately following the eruption (Figure 1).

Taken together, the back trajectories, radiance simulations, and return to typical retrieval quality confirm that the measured enhancements represent real volcanically enhanced H₂O values. However, the absolute magnitudes of the enhancements, especially for those failing the QS screening, are still in question because of the poor radiance fits. The MLS retrievals were not optimized to handle such strong H₂O enhancements. Thus, to fully quantify these injections and their uncertainties, we are developing a special retrieval for MLS measurements of the HT-HH plume. Preliminary results suggest that H₂O retrievals that better fit the radiances lie within 20% of current v4 estimates.

In addition, it is essential to account for the relatively coarse resolution of the MLS observations (~3.2 × 230 km for H₂O at these altitudes, as quantified by the averaging kernels (Livesey et al., 2020)) in the presence of strong vertically confined plumes (Schwartz et al., 2013, 2020). Accordingly, mid-January maximum plume values of 1500 ppmv measured by radiosondes (Sellitto et al., 2022) are not necessarily inconsistent with observed MLS abundances, given the disparity in their respective resolutions.

Many chemical species measured by MLS show anomalous mixing ratios in the plume (Figure S1 in Supporting Information S1). However, only the H₂O, SO₂, and HCl spectral signatures can confidently be ascribed to real enhancements in those quantities; perturbations in other species are likely artifacts arising from SO₂ spectral interference. SO₂ is retrieved from a spectrometer that targets an O¹⁸O line but also covers many SO₂ lines, the strongest of which are located in channels 5, 11, and 20. The triple-peak structure in measured radiances within the volcanic plume (Figure 2b) can only be plausibly explained by an SO₂ enhancement.

HCl is currently measured by a spectrometer that targets an O₃ line but covers HCl lines in channels 3 and 25. The ~5 K HCl radiance signature overlaps with an ~180 K O₃ signal. The differences between the measurements and the simulations with and without accounting for contributions from HCl reveal its expected ~5 K signature, suggesting that the observed enhancements represent real geophysical signals (Figure 2d). The HCl spectral signature is similar to that of the background because the HCl enhancements are not as dramatic as those of H₂O or SO₂.

MLS estimates of ice water content (IWC) are based on the differences between the measured radiances and the expected clear-sky radiances, with the residuals attributed to ice scattering and/or ice absorption. The clear-sky radiances are calculated using the retrieved atmospheric states; since most retrievals in the volcanic plume fail the QS in the days following the eruption, the derived IWC estimates are unreliable. In contrast, the quality of the MLS temperature, CO, and O₃ measurements is not affected by the plume.

3. Unprecedented Stratospheric H₂O Injection

Figure 3 compares the HT-HH HCl, SO₂, and H₂O stratospheric injections to other stratospheric injections (volcanic or otherwise) observed by MLS. Large injections are marked individually.

The HT-HH eruption did not inject vast amounts of either HCl or SO₂ into the stratosphere. The total injected mass of stratospheric SO₂ (calculated as described by Pumphrey et al. (2021)) was 0.41 ± 0.02 Tg, which pales in

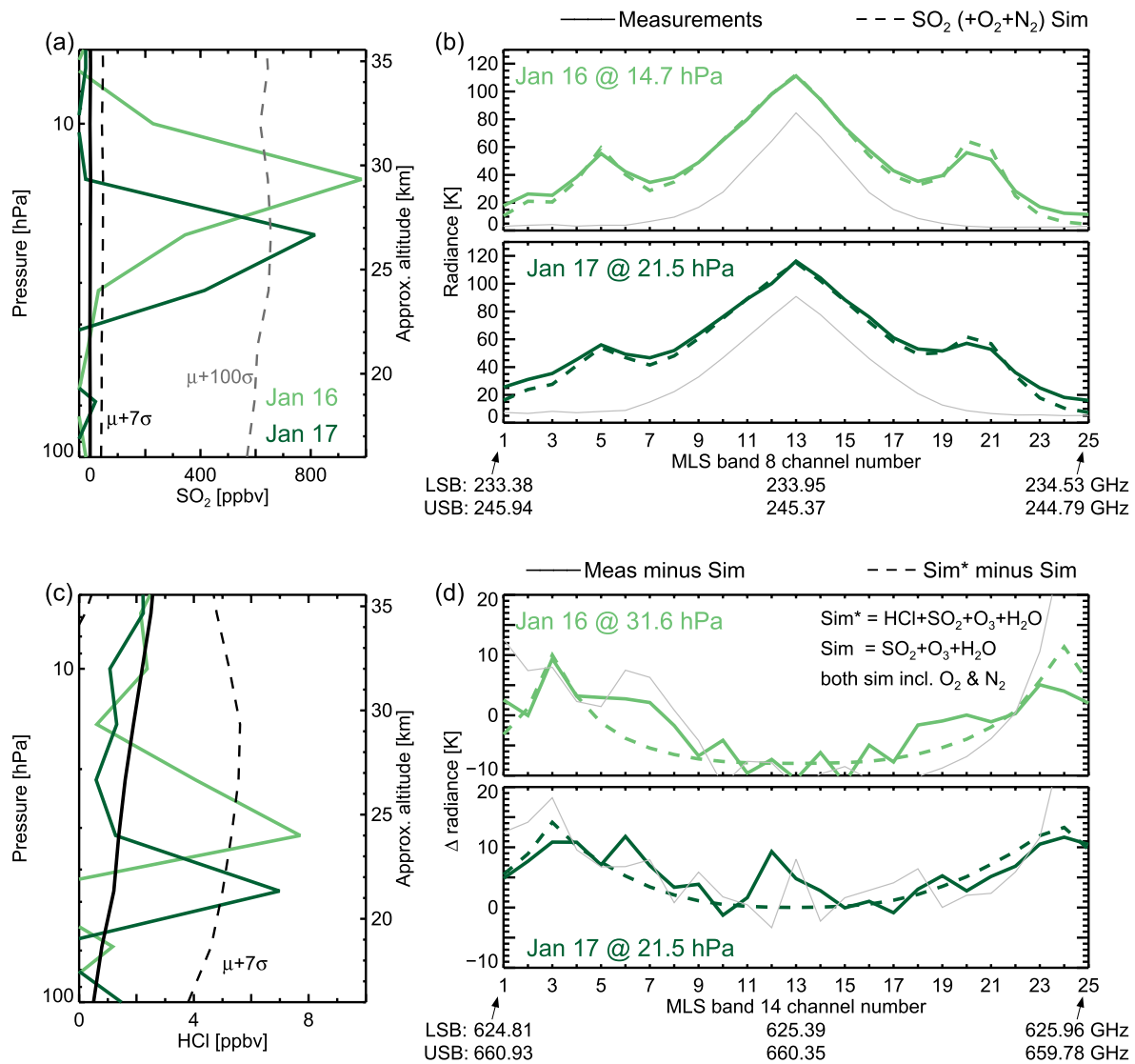


Figure 2. Profiles with maximum (a) SO₂ and (c) HCl on 16 and 17 January. All of these measurements lie downwind of the HT-HH volcano. (b) Measured (solid lines) and simulated (dashed) SO₂ radiances at the mixing ratio maxima for the enhanced profiles (colored lines) as well as for background conditions at the same pressure levels (gray lines). (d) Same as (b) but for differences between measured radiances and those simulated without HCl (solid lines) as well as estimated HCl signatures (from differences between simulations, see legend; dashed lines). All enhancements shown fail the QS.

comparison to that from previous eruptions measured by MLS, such as the 2008 Kasatochi, the 2009 Sarychev, or the 2019 Raikoke eruptions, which each emitted ~ 1 Tg (de Leeuw et al., 2021; Pumphrey et al., 2015). The mass of SO₂ injected by HT-HH is even less noteworthy in the context of the 17 Tg injected by the 1991 Pinatubo eruption (Read et al., 1993).

The only unusual aspect of the SO₂ plume is its injection height. SO₂ plumes are typically injected at altitudes no higher than 46 hPa (~ 21 km) (Carn et al., 2016; Pumphrey et al., 2015). HT-HH is the only injection observed by MLS that produced maximum values of SO₂ at 14 hPa (~ 29 km), with enhanced values detected up to 6.8 hPa (~ 35 km)—outside the normally recommended pressure range for MLS SO₂. By 27 January, the SO₂ plume dropped below background levels (Figure S1 in Supporting Information S1).

The HCl injection was similarly unremarkable, with only 8 profiles during 16–18 January (barely) exceeding the threshold for enhancement (Figure 2c; Figure S1 in Supporting Information S1). As with SO₂, the only unusual aspect of the HCl plume is its injection height of 31.6 hPa (~ 24 km), whereas previous eruptions reached no higher than 68 hPa (~ 18.6 km).

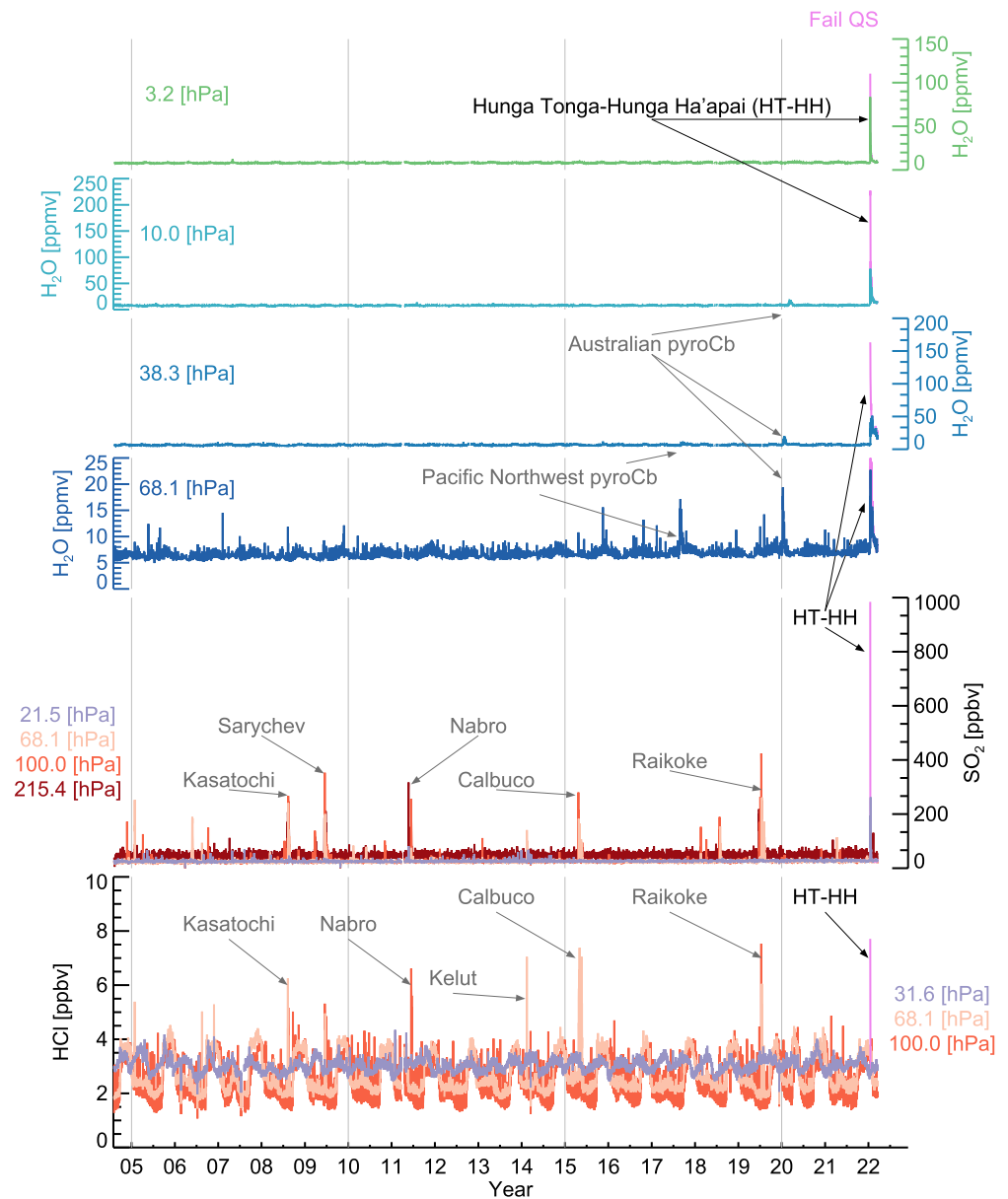


Figure 3. Time series of quality-screened maximum H_2O , SO_2 , and HCl mixing ratios at different pressure levels. SO_2 maxima at 14 hPa and HCl maxima at 31 hPa disregarding QS after the HT-HH eruption are shown in pink. Similarly, H_2O maxima disregarding QS are shown in pink for each level. Prior to the HT-HH eruption, we show QS data to avoid displaying retrieval artifacts, but no other injections failing the QS are found in the record.

In contrast, the magnitude of the HT-HH H_2O injection is unprecedented. Three natural pathways for direct injection of H_2O into the stratosphere exist: overshooting convection, pyrocumulonimbus (pyroCb) storms, and volcanic eruptions. The previous stratospheric H_2O record measured by MLS was 26.3 ppmv at 100 hPa associated with an overshooting convective event in August 2019 that spanned thousands of square kilometers and persisted for several hours (Werner et al., 2020). Two pyroCbs stand out in the MLS H_2O record: the 2017 Pacific Northwest (Pumphrey et al., 2021) and the 2019/2020 Australian New Year's (Kablick et al., 2020; Khaykin et al., 2020; Schwartz et al., 2020) events. Only the Australian pyroCbs injected enough H_2O to allow an accurate estimate of mass (19 ± 3 Tg).

The 2008 Kasatochi (Schwartz et al., 2013) and the 2015 Calbuco (Sioris et al., 2016) volcanic eruptions were the only others in the MLS record that injected appreciable amounts of H_2O into the stratosphere. Neither deposited

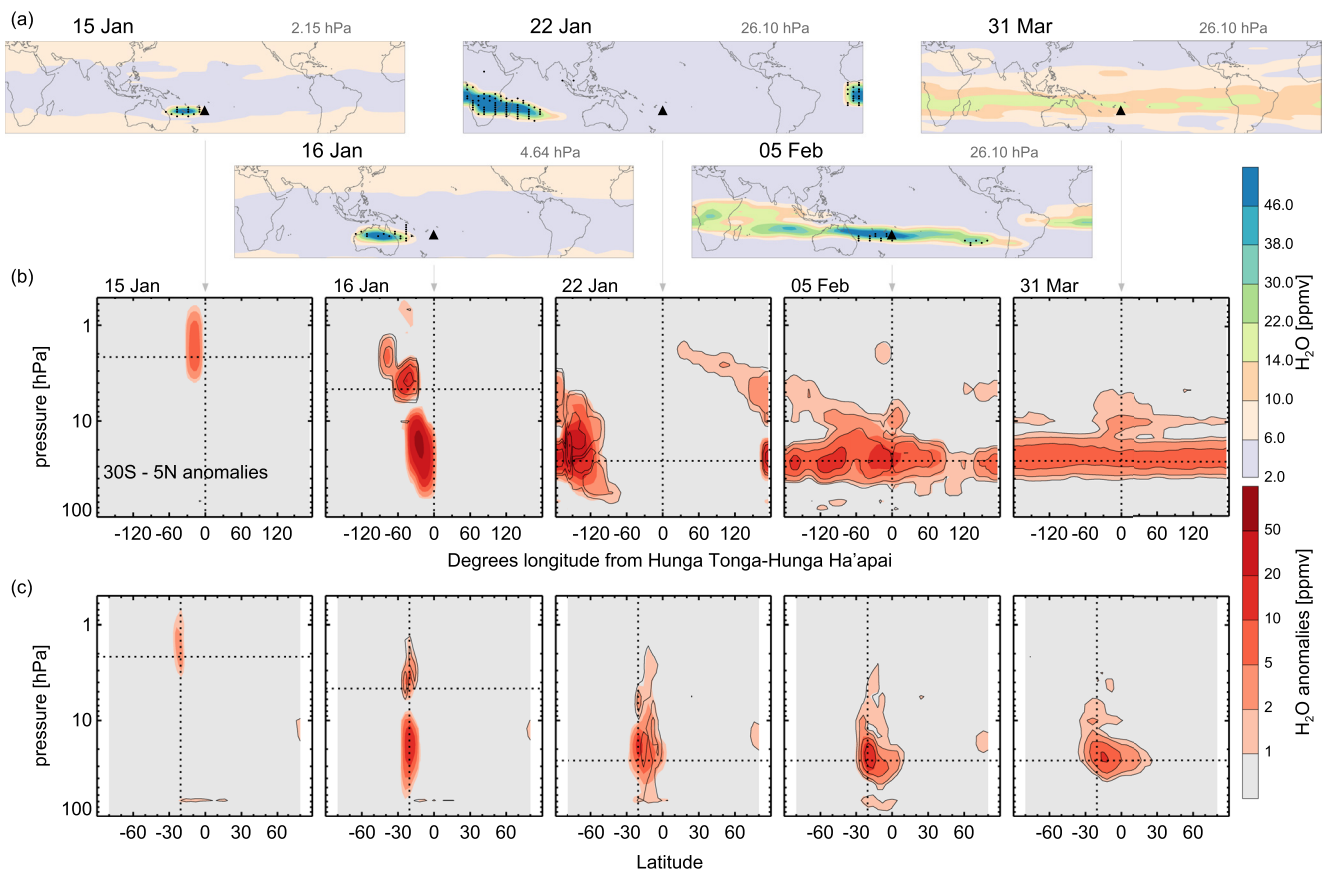


Figure 4. (a) Maps of H₂O at selected pressure levels for illustrative days after the eruption. Stippling indicates regions where a majority of the retrievals do not pass the QS. The volcano location is indicated by a triangle. (b) Meridional (30°S to 5°N) and (c) zonal mean anomalies for the same days. Colored contours show anomalies using all Microwave Limb Sounder H₂O retrievals, while line contours display the same anomalies based only on QS data; differences indicate regions where many measurements do not pass QS. The volcano location is shown by dashed vertical lines; dashed horizontal lines indicate the level of the map on each day.

H₂O at altitudes higher than 68 hPa (~18.6 km), and both injections were too small for a reliable H₂O mass estimate.

The HT-HH eruption injected at least 146 ± 5 Tg of H₂O into the stratosphere, not only surpassing the magnitudes of all other injections in the MLS record, but also eclipsing a theoretical estimate of 37.5 Tg from Pinatubo (Pitari & Mancini, 2002). This stratospheric H₂O injection is unique in the satellite record (1979 to date). To put the HT-HH injection into perspective, the enhancement represents ~10% of the estimated stratospheric H₂O burden of 1400 Tg (Glaze et al., 1997). Further, the H₂O plume injection height far exceeded that of any other injections in the MLS record (Figure 3).

4. Evolution of the H₂O Plume

To study the development of the H₂O plume, Figure 4 shows maps for selected days after the eruption and meridional and zonal mean anomalies based on all data points as well as only those that pass the QS criteria. On 15 January, the plume reached 0.46 hPa (~53 km), with most of the MLS retrievals failing QS. On 16 January, two separate plumes are visible, one in the upper stratosphere (between 1 and 8 hPa) and the other in the lower stratosphere (between 10 and 80 hPa), where most of the H₂O volume was injected. On this day, the effects on the plume of strong wind shear between 1 and 8 hPa are already apparent.

By 22 January, the plume had almost entirely circled the globe at 2.1 hPa, while only traveling halfway around at 26 hPa. On average, through January and February, the plume moved ~37° longitude per day at 2.1 hPa, but only ~18° longitude per day from 31 to 6 hPa, consistent with winds from meteorological analyses (see Figure S2 in Supporting Information S1) interpolated to the MLS measurement times and locations as described by Manney

et al. (2007). By 5 February, the plume covered all longitudes, with the largest enhancements from 38 to 21 hPa (~22–26 km). By 31 March, the plume around 4.6 hPa had dropped to near background values.

Measurements from 31 March show the persistence of the H₂O plume in the lower and middle stratosphere. Concurrent with encircling the globe, the H₂O plume broadened slowly, spreading mostly northward around 26 hPa. This plume will require further monitoring as the eruption signal propagates into the upper stratosphere and toward the poles in the Brewer-Dobson Circulation (BDC).

5. Discussion and Summary

The importance of stratospheric H₂O is well established; it affects stratospheric chemistry and dynamics as well as atmospheric radiation. For example, excess stratospheric H₂O could lead to enhanced OH concentrations, slightly enhancing O₃ production through the CH₄ oxidation cycle but worsening O₃ depletion through the HO_x cycle, leading to a net decrease in O₃ (e.g., Dvortsov & Solomon, 2001; Stenke & Grewe, 2005). The enhanced OH concentrations could also increase the loss of CH₄, resulting in a decrease in its lifetime (e.g., Ko et al., 2013; Stevenson et al., 2020) and thus reducing its long-term effect on climate. In addition, if enhanced H₂O concentrations were to be entrained into the developing Antarctic vortex to an extent sufficient to raise the formation temperature of polar stratospheric clouds, then the earlier onset of heterogeneous processing would exacerbate cumulative chemical O₃ loss. In terms of transport, a study of the dynamical response to a uniform doubling of stratospheric H₂O concluded that such moistening could reduce stratospheric temperature and increase the strength of the BDC; it could also result in the tropospheric westerly jets becoming stronger and storm tracks shifting poleward (Maycock et al., 2013). Since the HT-HH injection is ~10% of the stratospheric H₂O burden, a dynamical response of lesser magnitude than that found by Maycock et al. (2013) would be expected.

H₂O enters the stratosphere primarily in the tropics, where it freeze-dries at the cold point tropopause (Brewer, 1949). This mechanism gives rise to the “tape recorder,” whereby the annual cycle in tropopause temperatures is imprinted in alternating bands of dry and moist air rising in the tropical stratosphere (Mote et al., 1996). By short-circuiting the pathway through the cold point, HT-HH has disrupted this “heartbeat” signal (Figure 5a).

Consistent with the freeze-drying mechanism, unusually low tropopause temperatures around 2001 led to a sharp drop in the amount of H₂O entering the stratosphere (e.g., Randel et al., 2006; Rosenlof & Reid, 2008; Figure 5). This dry anomaly propagated via the BDC (Randel et al., 2006; Urban et al., 2014), slowly rising through the stratosphere and moving toward the poles. Using the propagation of the 2001 H₂O drop as described by Brinkop et al. (2016) as an analog for the transport of the HT-HH plume, we expect that ascent could carry volcanic H₂O to 10 hPa within ~9 months. The excess H₂O could arrive in northern and southern midlatitudes in ~18 and ~24 months, respectively, over a broad domain in the upper stratosphere. Since part of the plume has entered the lower branch of the BDC, the elevated H₂O may reach lower stratospheric midlatitudes within a few months. The timescale for complete dissipation of the plume may be 5–10 years (Hall & Waugh, 1997).

Radiative calculations of the sudden drop in H₂O of ~0.4 ppmv (at 100 hPa) in 2001 (Figure 5b) demonstrated that the radiative forcing from even small variations in lower stratospheric H₂O could induce decadal-scale changes in global-mean surface temperature (e.g., Solomon et al., 2010). The unprecedented HT-HH enhancement would correspond to ~1.5 ppmv (at 31 hPa) if averaged over 60°S–60°N.

Previous studies of the radiative effects of stratospheric H₂O perturbations, including direct volcanic injection, have shown that they can cause surface warming (e.g., Joshi & Jones, 2009; Rind & Lonergan, 1995). As established in Section 3, the HT-HH eruption was unusual in that it injected extremely large amounts of H₂O. Preliminary climate model simulations (see Supporting Information S1 for details) suggest an effective radiative forcing (e.g., Forster et al., 2001; Myhre et al., 2013; Smith et al., 2020; Wang et al., 2017) at the tropopause of +0.15 Wm⁻² due to the stratospheric H₂O enhancement (Figure S3b in Supporting Information S1). For comparison, the radiative forcing increase due to the CO₂ growth from 1996 to 2005 was about +0.26 Wm⁻² (Solomon et al., 2010).

The HT-HH H₂O enhancement will exert a positive radiative forcing on the surface, offsetting the surface cooling caused by the aerosol radiative forcing (e.g., Sellitto et al., 2022; Zhang et al., 2022). Given the extraordinary magnitude of the HT-HH H₂O injection and the fact that its anticipated stratospheric residence time exceeds the typical 2–3 years timescale for sulfate aerosols to fall out of the stratosphere (Joshi & Jones, 2009), HT-HH may

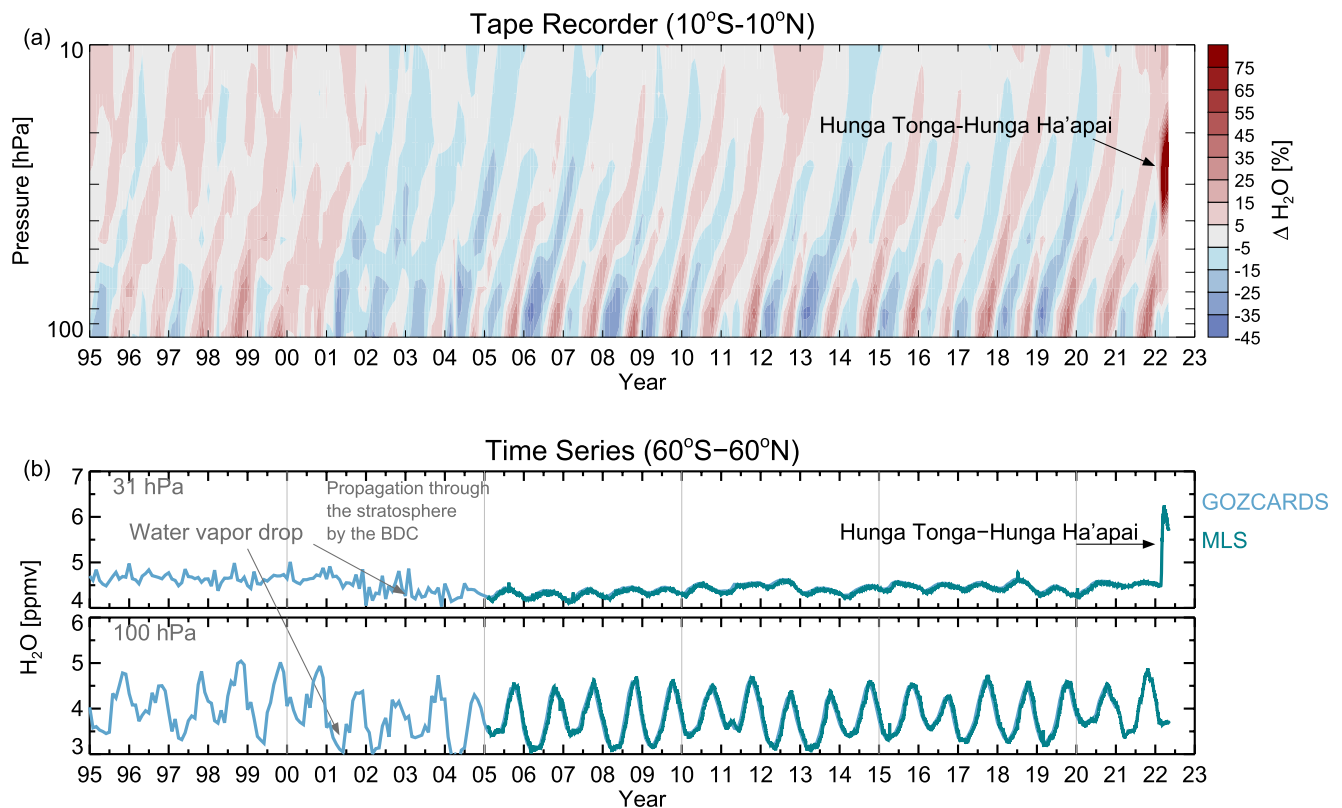


Figure 5. (a) The atmospheric tape recorder (zonal mean H_2O anomalies in the tropics). (b) Time series of near-global (60°S to 60°N) H_2O at 100 and 31 hPa. H_2O abundances are based on GOZCARDS (Froidevaux et al., 2015) and Microwave Limb Sounder data.

be the first volcanic eruption observed to impact climate not through surface cooling caused by volcanic sulfate aerosols, but rather through surface warming caused by excess H_2O radiative forcing.

In summary, MLS measurements indicate that an exceptional amount of H_2O was injected directly into the stratosphere by the HT-HH eruption. We estimate that the magnitude of the injection constituted at least 10% of the total stratospheric H_2O burden. On the day of the eruption, the H_2O plume reached ~ 53 km altitude. The H_2O injection bypassed the cold point tropopause, disrupted the H_2O tape recorder signal, set a new record for H_2O injection height in the 17-year MLS record, and could alter stratospheric chemistry and dynamics as the long-lived H_2O plume propagates through the stratosphere in the BDC. Unlike previous strong eruptions in the satellite era, HT-HH could impact climate not through surface cooling due to sulfate aerosols, but rather through surface warming due to the excess stratospheric H_2O forcing. Given the potential high-impact consequences of the HT-HH H_2O injection, it is critical to continue monitoring volcanic gases from this eruption and future ones to better quantify their varying roles in climate.

Data Availability Statement

The data sets used here are publicly available as follows. Aura MLS Level 2 data: <https://disc.gsfc.nasa.gov/datasets?page=1&keywords=AURA%20MLS>; Aura MLS Derived Meteorological Products: <https://mls.jpl.nasa.gov/eos-aura-mls/dmp> (registration required).

References

- Brewer, A. W. (1949). Evidence for a world circulation provided by the measurements of helium and water vapour distribution in the stratosphere. *Quarterly Journal of the Royal Meteorological Society*, 75(326), 351–363. <https://doi.org/10.1002/qj.49707532603>
- Brinkop, S., Dameris, M., Jöckel, P., Garny, H., Lossow, S., & Stiller, G. (2016). The millennium water vapour drop in chemistry–climate model simulations. *Atmospheric Chemistry and Physics*, 16(13), 8125–8140. <https://doi.org/10.5194/acp-16-8125-2016>

Acknowledgments

The research was carried out at the Jet Propulsion Laboratory (JPL), California Institute of Technology, under a contract with the National Aeronautics and Space Administration (80NM0018D0004). GLM was supported by the JPL Microwave Limb Sounder team under JPL subcontract #1521127 to NWRA. We thank S. Khaykin for helpful discussions. The suggestions for improvements from the two anonymous reviewers are gratefully acknowledged.

- Carn, S., Clarisse, L., & Prata, A. (2016). Multi-decadal satellite measurements of global volcanic degassing. *Journal of Volcanology and Geothermal Research*, 311, 99–134. <https://doi.org/10.1016/j.jvolgeores.2016.01.002>
- Carr, J. L., Horvath, A., Wu, D. L., & Friberg, M. D. (2022). Stereo plume height and motion retrievals for the record-setting Hunga Tonga-Hunga Ha'apai eruption of 15 January 2022. *Geophysical Research Letters*, 49(9), e2022GL098131. <https://doi.org/10.1029/2022GL098131>
- Carvajal, M., Sepúlveda, I., Gubler, A., & Garreaud, R. (2022). Worldwide signature of the 2022 Tonga volcanic tsunami. *Geophysical Research Letters*, 49(6). <https://doi.org/10.1029/2022gl098153>
- Coffey, M. T. (1996). Observations of the impact of volcanic activity on stratospheric chemistry. *Journal of Geophysical Research*, 101(D3), 6767–6780. <https://doi.org/10.1029/95jd03763>
- Cronin, S., Brenna, M., Smith, I., Barker, S., Tost, M., Ford, M., et al. (2017). *New volcanic island unveils explosive past*. Eos. <https://doi.org/10.1029/2017eo076589>
- de Leeuw, J., Schmidt, A., Witham, C. S., Theys, N., Taylor, I. A., Grainger, R. G., et al. (2021). The 2019 Raikoke volcanic eruption—Part 1: Dispersion model simulations and satellite retrievals of volcanic sulfur dioxide. *Atmospheric Chemistry and Physics*, 21(14), 10851–10879. <https://doi.org/10.5194/acp-21-10851-2021>
- Dvortsov, V. L., & Solomon, S. (2001). Response of the stratospheric temperatures and ozone to past and future increases in stratospheric humidity. *Journal of Geophysical Research*, 106(D7), 7505–7514. <https://doi.org/10.1029/2000jd900637>
- Forster, P. M., Ponater, M., & Zhong, W.-Y. (2001). Testing broadband radiation schemes for their ability to calculate the radiative forcing and temperature response to stratospheric water vapour and ozone changes. *Meteorologische Zeitschrift*, 10(5), 387–393. <https://doi.org/10.1127/0941-2948/2001/0010-0387>
- Froidevaux, L., Anderson, J., Wang, H.-J., Fuller, R. A., Schwartz, M. J., Santee, M. L., et al. (2015). Global OZone chemistry and related trace gas data records for the stratosphere (GOZCARDS): Methodology and sample results with a focus on HCl, H₂O, and O₃. *Atmospheric Chemistry and Physics*, 15(18), 10471–10507. <https://doi.org/10.5194/acp-15-10471-2015>
- Glaze, L. S., Baloga, S. M., & Wilson, L. (1997). Transport of atmospheric water vapor by volcanic eruption columns. *Journal of Geophysical Research*, 102(D5), 6099–6108. <https://doi.org/10.1029/96jd03125>
- Hall, T. M., & Waugh, D. (1997). Tracer transport in the tropical stratosphere due to vertical diffusion and horizontal mixing. *Geophysical Research Letters*, 24(11), 1383–1386. <https://doi.org/10.1029/97gl01289>
- Joshi, M. M., & Jones, G. S. (2009). The climatic effects of the direct injection of water vapour into the stratosphere by large volcanic eruptions. *Atmospheric Chemistry and Physics*, 9(16), 6109–6118. <https://doi.org/10.5194/acp-9-6109-2009>
- Kablick, G. P., Allen, D. R., Fromm, M. D., & Nedoluha, G. E. (2020). Australian PyroCb smoke generates synoptic-scale stratospheric anticyclones. *Geophysical Research Letters*, 47(13), e2020GL088101. <https://doi.org/10.1029/2020GL088101>
- Khaykin, S., Legras, B., Bucci, S., Sellitto, P., Isaksen, I., Tencé, F., et al. (2020). The 2019/20 Australian wildfires generated a persistent smoke-charged vortex rising up to 35 km altitude. *Communications Earth and Environment*, 1(1), 22. <https://doi.org/10.1038/s43247-020-00022-5>
- Ko, M. K. W., Newman, P. A., Reimann, S., & Strahan, S. E. (Eds.). (2013). *SPARC report on lifetimes of stratospheric ozone-depleting substances, their replacements, and related species*, SPARC (Vol. No. 6, Tech. Rep.). Retrieved from <http://www.sparc-climate.org/publications/sparc-reports/>
- Kusky, T. M. (2022). Déjà vu: Might future eruptions of Hunga Tonga-Hunga Ha'apai volcano be a repeat of the devastating eruption of Santorini, Greece (1650 BC)? *Journal of Earth Sciences*, 33(2), 229–235. <https://doi.org/10.1007/s12583-022-1624-2>
- Livesey, N. J., Read, W., Wagner, L., Froidevaux, P. A., Lambert, A., Manney, G. L., et al. (2020). Version 4.2x Level 2 and 3 data quality and description document (Tech. Rep. No. JPL D-33509 Rev. E). *Jet Propulsion Laboratory*. Retrieved from <http://mils.jpl.nasa.gov>
- Livesey, N. J., Santee, M. L., & Manney, G. L. (2015). A Match-based approach to the estimation of polar stratospheric ozone loss using Aura Microwave Limb Sounder observations. *Atmospheric Chemistry and Physics*, 15(17), 9945–9963. <https://doi.org/10.5194/acp-15-9945-2015>
- Livesey, N. J., Snyder, W. V., Read, W. G., & Wagner, P. A. (2006). Retrieval algorithms for the EOS Microwave Limb Sounder (MLS). *IEEE Transactions on Geoscience and Remote Sensing*, 44(5), 1144–1155. <https://doi.org/10.1109/tgrs.2006.872327>
- Manney, G. L., Daffer, W. H., Zawodny, J. M., Bernath, P. F., Hoppel, K. W., Walker, K. A., et al. (2007). Solar occultation satellite data and derived meteorological products: Sampling issues and comparisons with Aura Microwave Limb Sounder. *Journal of Geophysical Research*, 112(D24), D24S50. <https://doi.org/10.1029/2007jd008709>
- Maycock, A. C., Joshi, M. M., Shine, K. P., & Scaife, A. A. (2013). The circulation response to idealized changes in stratospheric water vapor. *Journal of Climate*, 26(2), 545–561. <https://doi.org/10.1175/jcli-d-12-00155.1>
- McCormick, M. P., Thomason, L. W., & Trepte, C. R. (1995). Atmospheric effects of the Mt Pinatubo eruption. *Nature*, 373(6513), 399–404. <https://doi.org/10.1038/373399a0>
- Mote, P. W., Rosenlof, K. H., McIntyre, M. E., Carr, E. S., Gille, J. C., Holton, J. R., et al. (1996). An atmospheric tape recorder: The imprint of tropical tropopause temperatures on stratospheric water vapor. *Journal of Geophysical Research*, 101(D2), 3989–4006. <https://doi.org/10.1029/95jd03422>
- Myhre, G., Shindell, D., Bréon, F.-M., Collins, W., Fuglestedt, J., Huang, J., et al. (2013). Anthropogenic and natural radiative forcing. In T. F. Stocker, D. Qin, G.-K. Plattner, M. Tignor, S. K. Allen, J. Boschung, et al. (Eds.), *Climate change 2013: The physical science basis. Contribution of working group I to the fifth assessment report of the Intergovernmental Panel on Climate Change* (pp. 659–740). Cambridge University Press. <https://doi.org/10.1017/CBO9781107415324.018>
- Pinto, J. P., Turco, R. P., & Toon, O. B. (1989). Self-limiting physical and chemical effects in volcanic eruption clouds. *Journal of Geophysical Research*, 94(D8), 11165. <https://doi.org/10.1029/jd094id08p11165>
- Pitari, G., & Mancini, E. (2002). Short-term climatic impact of the 1991 volcanic eruption of Mt. Pinatubo and effects on atmospheric tracers. *Natural Hazards and Earth System Sciences*, 2(1/2), 91–108. <https://doi.org/10.5194/nhess-2-91-2002>
- Proud, S. R., Prata, A., & Schmauss, S. (2022). The January 2022 eruption of Hunga Tonga-Hunga Ha'apai volcano reached the mesosphere. *Earth and Space Science Open Archive*, 11. <https://doi.org/10.1002/essoar.10511092.1>
- Pumphrey, H. C., Read, W. G., Livesey, N. J., & Yang, K. (2015). Observations of volcanic SO₂ from MLS on Aura. *Atmospheric Measurement Techniques*, 8(1), 195–209. <https://doi.org/10.5194/amt-8-195-2015>
- Pumphrey, H. C., Schwartz, M. J., Santee, M. L., Kablick, G. P., Fromm, M. D., & Livesey, N. J. (2021). Microwave Limb Sounder (MLS) observations of biomass burning products in the stratosphere from Canadian forest fires in August 2017. *Atmospheric Chemistry and Physics*, 21(22), 16645–16659. <https://doi.org/10.5194/acp-21-16645-2021>
- Ramirez-Herrera, M. T., Coca, O., & Vargas-Espinosa, V. (2022). Tsunami effects on the Coast of Mexico by the Hunga Tonga-Hunga Ha'apai volcano eruption. *Pure and Applied Geophysics*, 179, 1117–1137. <https://doi.org/10.31223/x5x33z>

- Randel, W. J., Wu, F., Vömel, H., Nedoluha, G. E., & Forster, P. (2006). Decreases in stratospheric water vapor after 2001: Links to changes in the tropical tropopause and the Brewer-Dobson circulation. *Journal of Geophysical Research*, *111*(D12), D12312. <https://doi.org/10.1029/2005jd006744>
- Read, W. G., Froidevaux, L., & Waters, J. W. (1993). Microwave Limb Sounder measurement of stratospheric SO₂ from the Mt. Pinatubo volcano. *Geophysical Research Letters*, *20*(12), 1299–1302. <https://doi.org/10.1029/93gl00831>
- Rind, D., & Loneragan, P. (1995). Modeled impacts of stratospheric ozone and water vapor perturbations with implications for high-speed civil transport aircraft. *Journal of Geophysical Research*, *100*(D4), 7381–7396. <https://doi.org/10.1029/95jd00196>
- Rosenlof, K. H., & Reid, G. C. (2008). Trends in the temperature and water vapor content of the tropical lower stratosphere: Sea surface connection. *Journal of Geophysical Research*, *113*(D6), D06107. <https://doi.org/10.1029/2007jd009109>
- Santee, M. L., Lambert, A., Manney, G. L., Livesey, N. J., Froidevaux, L., Neu, J. L., et al. (2022). Prolonged and pervasive perturbations in the composition of the Southern Hemisphere midlatitude lower stratosphere from the Australian New Year's fires. *Geophysical Research Letters*, *49*(4), e2021GL096270. <https://doi.org/10.1029/2021GL096270>
- Schwartz, M. J., Read, W. G., Santee, M. L., Livesey, N. J., Froidevaux, L., Lambert, A., & Manney, G. L. (2013). Convectively injected water vapor in the North American summer lowermost stratosphere. *Geophysical Research Letters*, *40*(10), 2316–2321. <https://doi.org/10.1002/grl.50421>
- Schwartz, M. J., Santee, M. L., Pumphrey, H. C., Manney, G. L., Lambert, A., Livesey, N. J., et al. (2020). Australian New Year's pyroCb impact on stratospheric composition. *Geophysical Research Letters*, *47*(24). <https://doi.org/10.1029/2020gl090831>
- Sellitto, P., Podglajen, A., Belhadji, R., Boichu, M., Carboni, E., Cuesta, J., et al. (2022). The unexpected radiative impact of the Hunga Tonga eruption of January 15th, 2022. <https://doi.org/10.21203/rs.3.rs-1562573/v1>
- Sioris, C. E., Malo, A., McLinden, C. A., & D'Amours, R. (2016). Direct injection of water vapor into the stratosphere by volcanic eruptions. *Geophysical Research Letters*, *43*(14), 7694–7700. <https://doi.org/10.1002/2016gl069918>
- Smith, C. J., Kramer, R. J., Myhre, G., Alterskjær, K., Collins, W., Sima, A., et al. (2020). Effective radiative forcing and adjustments in CMIP6 models. *Atmospheric Chemistry and Physics*, *20*(16), 9591–9618. <https://doi.org/10.5194/acp-20-9591-2020>
- Solomon, S., Rosenlof, K. H., Portmann, R. W., Daniel, J. S., Davis, S. M., Sanford, T. J., & Plattner, G.-K. (2010). Contributions of stratospheric water vapor to decadal changes in the rate of global warming. *Science*, *327*(5970), 1219–1223. <https://doi.org/10.1126/science.1182488>
- Stenke, A., & Grewe, V. (2005). Simulation of stratospheric water vapor trends: Impact on stratospheric ozone chemistry. *Atmospheric Chemistry and Physics*, *5*(5), 1257–1272. <https://doi.org/10.5194/acp-5-1257-2005>
- Stevenson, D. S., Zhao, A., Naik, V., O'Connor, F. M., Tilmes, S., Zeng, G., et al. (2020). Trends in global tropospheric hydroxyl radical and methane lifetime since 1850 from AerChemMIP. *Atmospheric Chemistry and Physics*, *20*(21), 12905–12920. <https://doi.org/10.5194/acp-20-12905-2020>
- Themens, D. R., Watson, C., Žagar, N., Vasylykevych, S., Elvidge, S., McCaffrey, A., et al. (2022). Global propagation of ionospheric disturbances associated with the 2022 Tonga volcanic eruption. *Geophysical Research Letters*, *49*(7). <https://doi.org/10.1029/2022gl098158>
- Urban, J., Lossow, S., Stiller, G., & Read, W. (2014). Another drop in water vapor. *Eos, Transactions American Geophysical Union*, *95*(27), 245–246. <https://doi.org/10.1002/2014eo270001>
- Wang, Y., Su, H., Jiang, J. H., Livesey, N. J., Santee, M. L., Froidevaux, L., et al. (2017). The linkage between stratospheric water vapor and surface temperature in an observation-constrained coupled general circulation model. *Climate Dynamics*, *48*(7–8), 2671–2683. <https://doi.org/10.1007/s00382-016-3231-3>
- Waters, J., Froidevaux, L., Harwood, R., Jarnot, R., Pickett, H., Read, W., et al. (2006). The Earth Observing System Microwave Limb Sounder (EOS MLS) on the Aura satellite. *IEEE Transactions on Geoscience and Remote Sensing*, *44*(5), 1075–1092. <https://doi.org/10.1109/tgrs.2006.873771>
- Werner, F., Schwartz, M. J., Livesey, N. J., Read, W. G., & Santee, M. L. (2020). Extreme outliers in lower stratospheric water vapor over North America observed by MLS: Relation to overshooting convection diagnosed from collocated Aqua-MODIS data. *Geophysical Research Letters*, *47*(24). <https://doi.org/10.1029/2020gl090131>
- Wright, C., Hindley, N., Alexander, M. J., Barlow, M., Hoffmann, L., Mitchell, C., et al. (2022). Surface-to-space atmospheric waves from Hunga Tonga-Hunga Ha'apai eruption. *Earth and Space Science Open Archive*, *23*. <https://doi.org/10.1002/essoar.10510674.2>
- Yuen, D. A., Scruggs, M. A., Spera, F. J., Zheng, Y., Hu, H., McNutt, S. R., et al. (2022). Under the surface: Pressure-induced planetary-scale waves, volcanic lightning, and gaseous clouds caused by the submarine eruption of Hunga Tonga-Hunga Ha'apai volcano. *Earthquake Research Advances*, 100134. <https://doi.org/10.1016/j.eqrea.2022.100134>
- Zhang, H., Wang, F., Li, J., Duan, Y., Zhu, C., & He, J. (2022). Potential impact of Tonga volcano eruption on global mean surface air temperature. *Journal of Meteorological Research*, *36*(1), 1–5. <https://doi.org/10.1007/s13351-022-2013-6>